Supplementary Information of

Lanthanide (III) Coordination Polymers for Luminescent Detection of Fe (III) and Picric Acid

Cong Xu[a], Haipeng Huang[a], Jingxin Ma[b], Wei Liu[a], Chunyang Chen[a], Xin Huang[a], Lizi Yang[a], Fu-Xing Pan[a], and Weisheng Liu[a,*]

a. Key Laboratory of Nonferrous Metals Chemistry and Resources Utilization of Gansu Province and State Key Laboratory of Applied Organic Chemistry, College of Chemistry and Chemical Engineering, Lanzhou University, Lanzhou 730000, P. R. China
Email: liuws@lzu.edu.cn Tel: +86 931-8915151

b. College of Chemistry and Chemical Engineering, Ningxia University, Yinchuan 750021, P.R. China.

Content

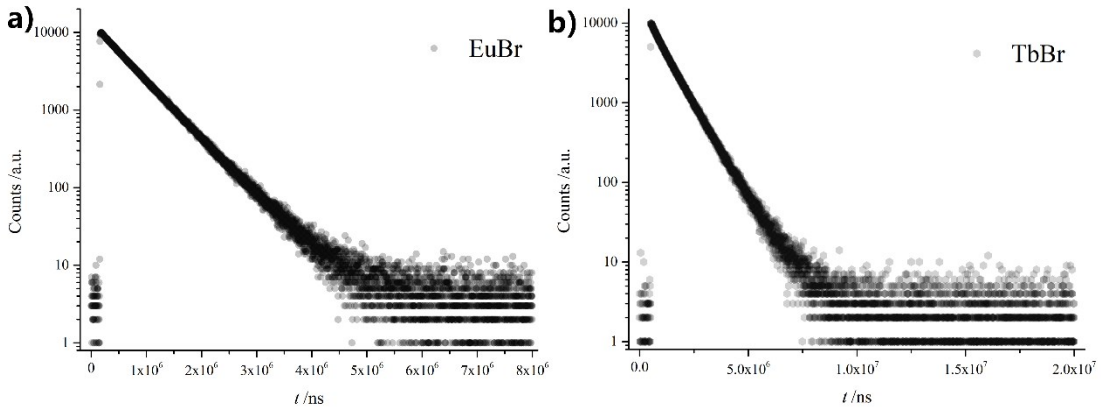

Figure S1. Luminescence lifetime decay profiles of **a) EuBr** and **b) TbBr.**

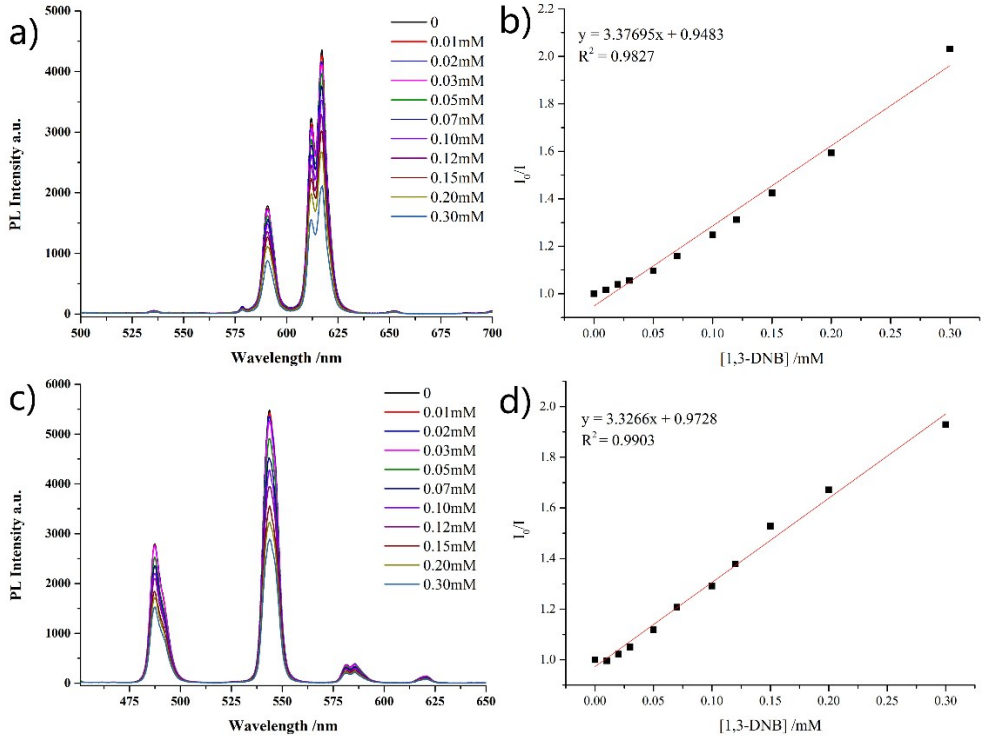

Figure S2. a) The Emission of **EuBr** with different concentrations of 1,3-Dinitrobenzene. b) The Stern-Volmer (SV) plot of I_o/I versus increasing concentrations of 1,3-Dinitrobenzene. c) The Emission of **TbBr** with different concentrations of 1,3-Dinitrobenzene. d) The Stern-Volmer (SV) plot of I_o/I versus increasing concentrations of 1,3-Dinitrobenzene.

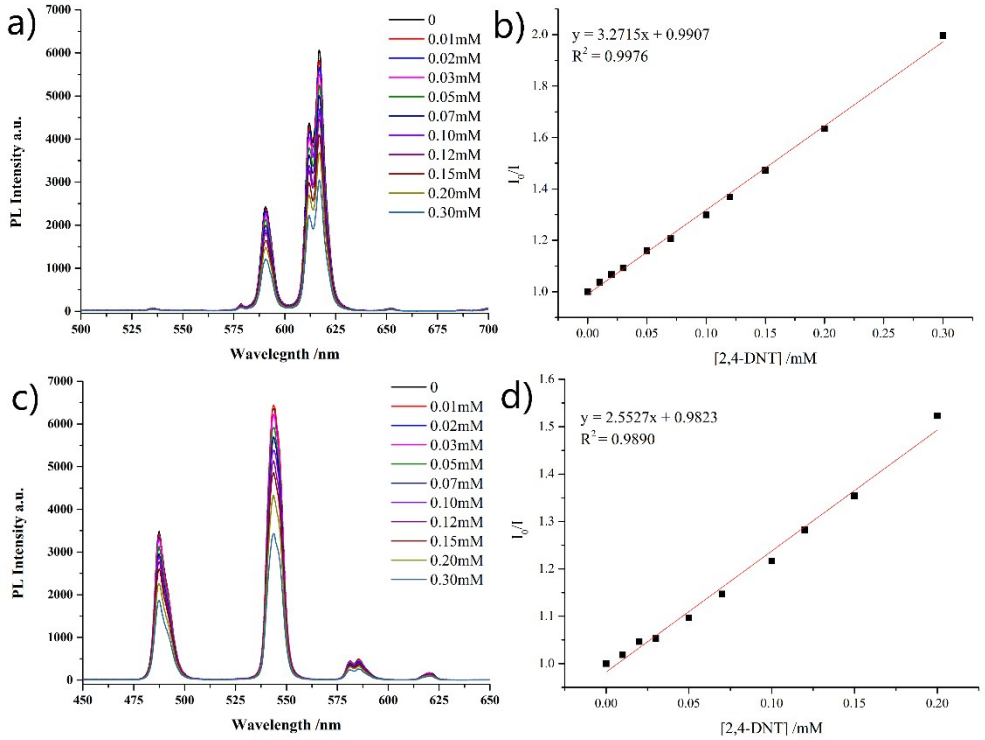

Figure S3. a) The Emission of **EuBr** with different concentrations of 2,4-Dinitrotoluene. b) The Stern-Volmer (SV) plot of I_o/I versus increasing concentrations of 2,4-Dinitrotoluene. c) The Emission of **TbBr** with different concentrations of 2,4-Dinitrotoluene. d) The Stern-Volmer (SV) plot of I_o/I versus increasing concentrations of 2,4-Dinitrotoluene.

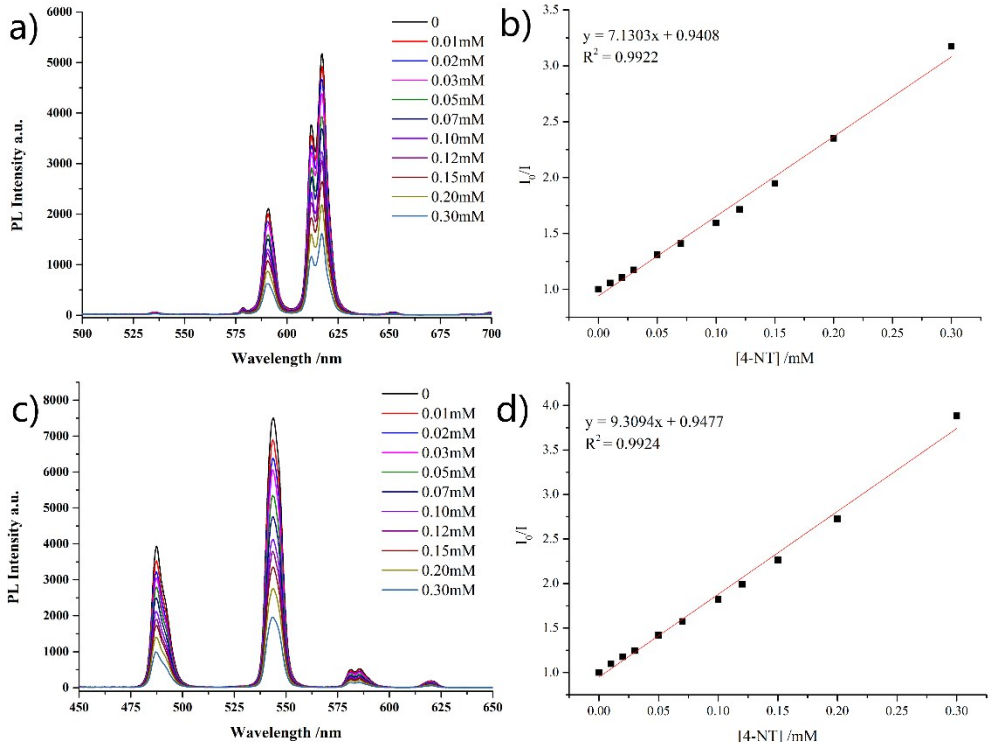

Figure S4. a) The Emission of **EuBr** with different concentrations of 4-Nitrotoluene. b) The Stern-Volmer (SV) plot of I_o/I versus increasing concentrations of 4-Nitrotoluene.) The Emission of **EuBr** with different concentrations of 4-Nitrotoluene. d) The Stern-Volmer (SV) plot of I_o/I versus increasing concentrations of 4-Nitrotoluene.

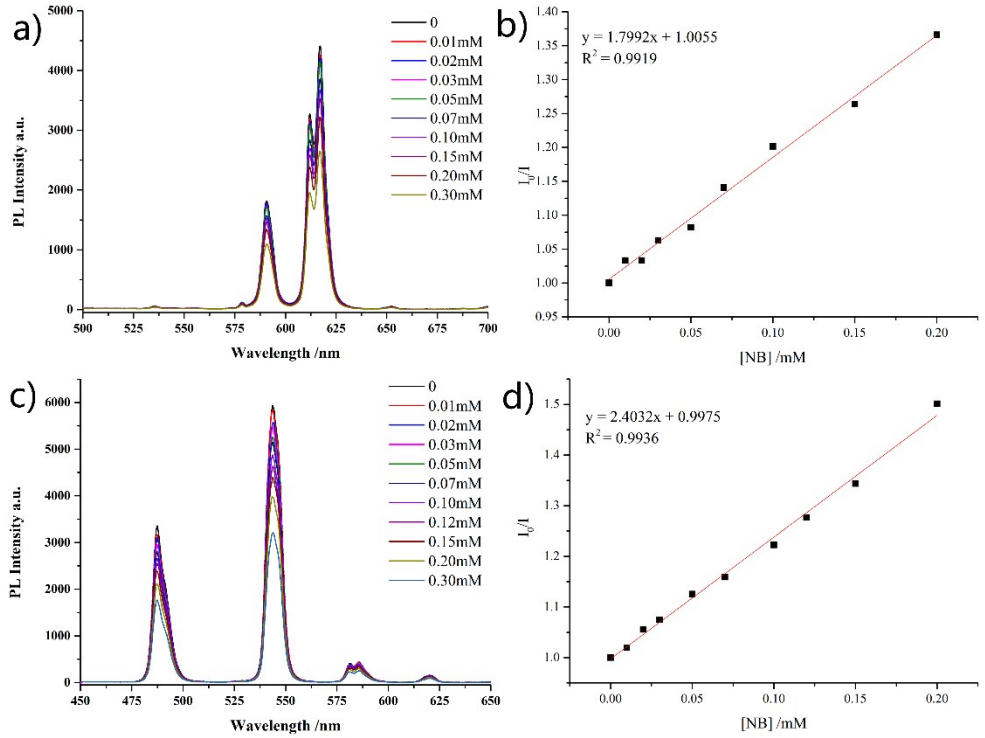

Figure S5. a) The Emission of **EuBr** with different concentrations of Nitrobenzene. b) The Stern-Volmer (SV) plot of I_o/I versus increasing concentrations of Nitrobenzene. c) The Emission of **TbBr** with different concentrations of Nitrobenzene. d) The Stern-Volmer (SV) plot of I_o/I versus increasing concentrations of Nitrobenzene.

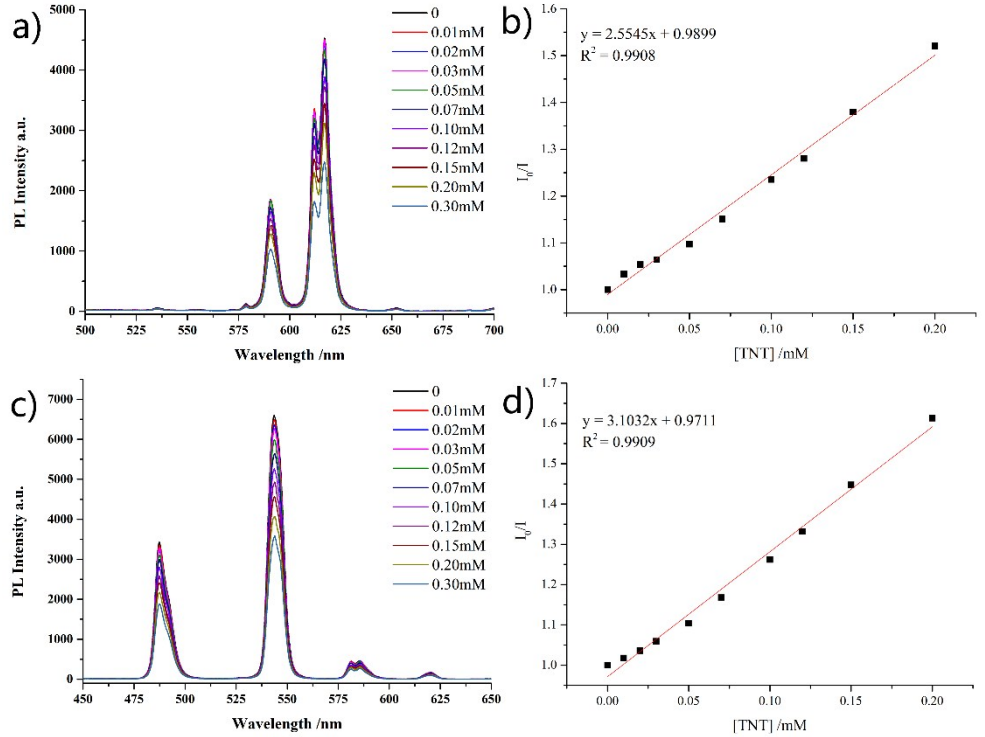

Figure S6. a) The Emission of **EuBr** with different concentrations of 2,4,6-Trinitrotoluene. b) The Stern-Volmer (SV) plot of I_o/I versus increasing concentrations of 2,4,6-Trinitrotoluene. c) The Emission of **TbBr** with different concentrations of 2,4,6-Trinitrotoluene. d) The Stern-Volmer (SV) plot of I_o/I versus increasing concentrations of 2,4,6-Trinitrotoluene.

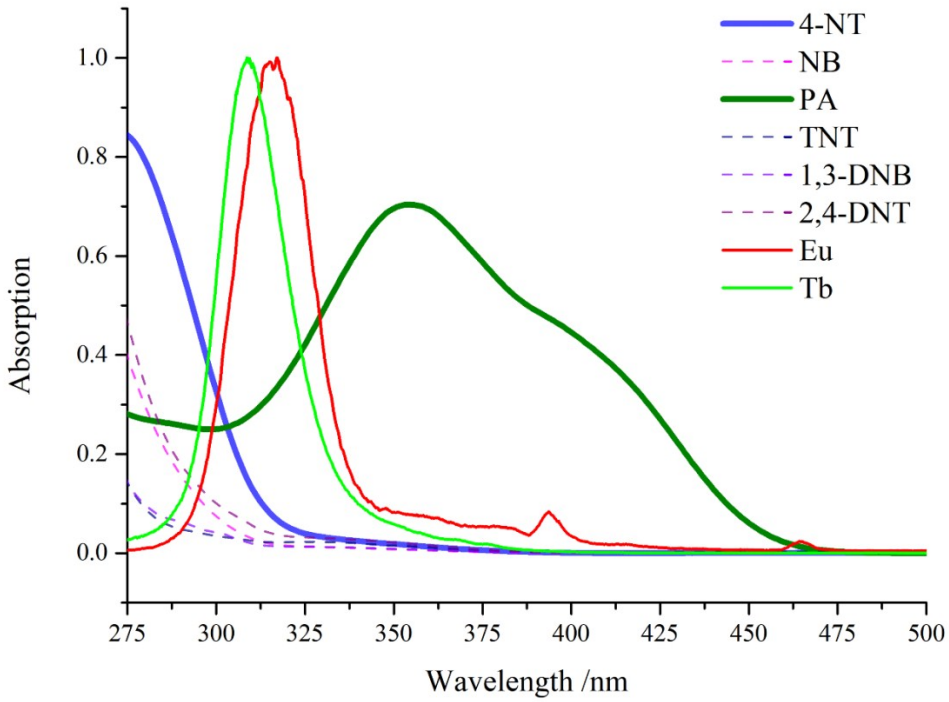

Figure S7. The spectral overlap between normalized excitation spectrum of **EuBr** and **TbBr** and normalized absorbance spectra of nitro explosives.

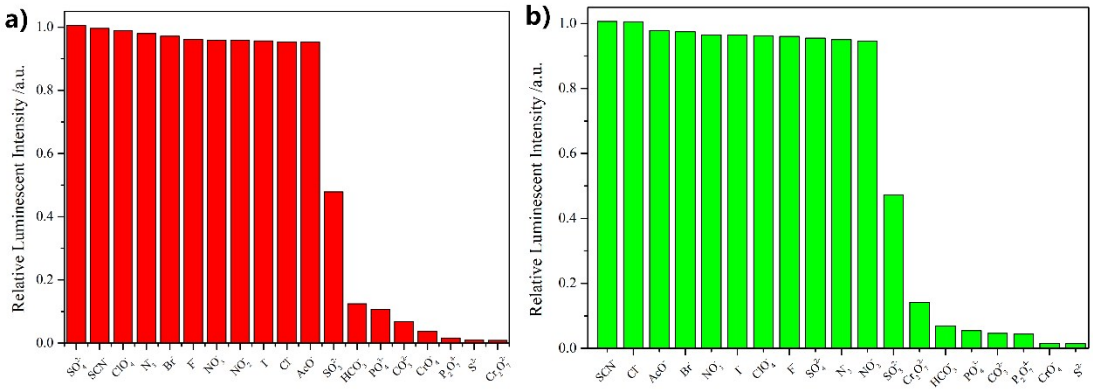

Figure S8. Anion selectivity of **a) EuBr** and **b) TbBr** (I_0/I, 1mM) in water.

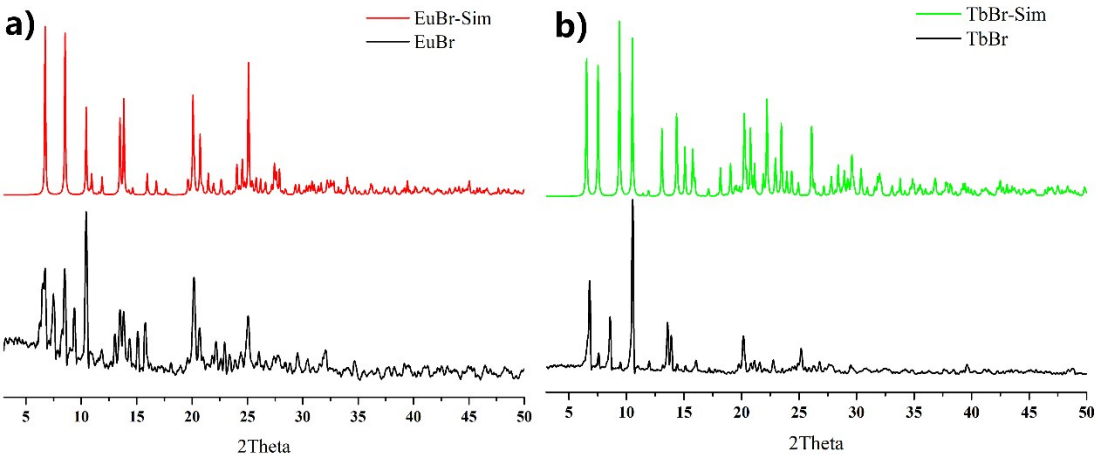

Figure S9. The PXRD patterns of **EuBr** and **TbBr**.

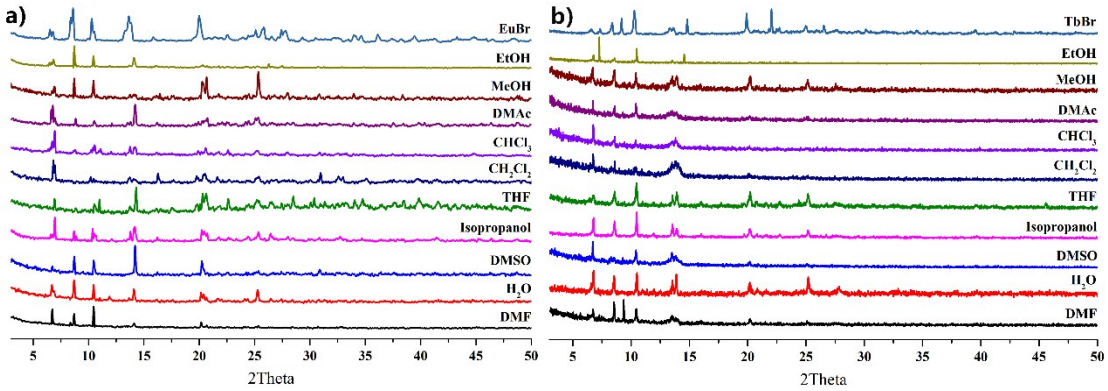

Figure S10. The PXRD patterns of **a) EuBr** and **b) TbBr** treated by various solvent for 24h.

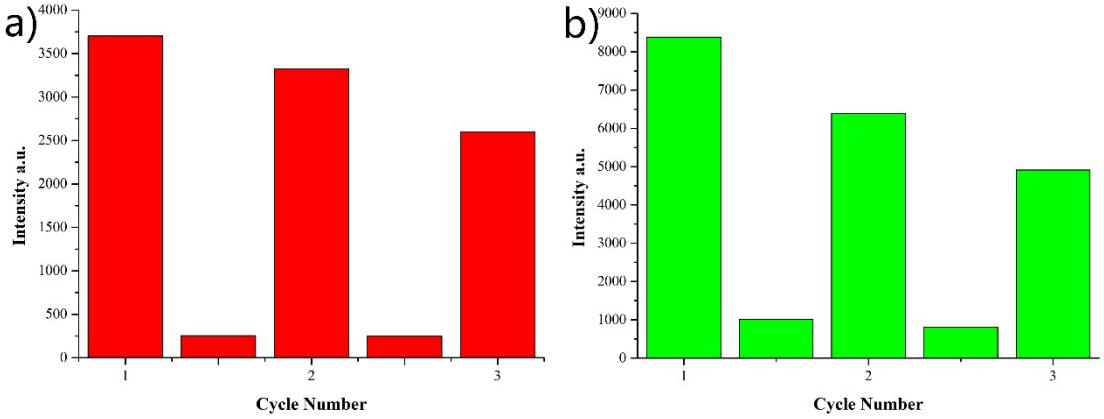

Figure S11. Reproducibility of the quenching ability of a) **EuBr** 617nm and b) **TbBr** 544nm in water and in the presence of 0.5mM PA (ex= 317nm for EuBr, 309nm for TbBr).

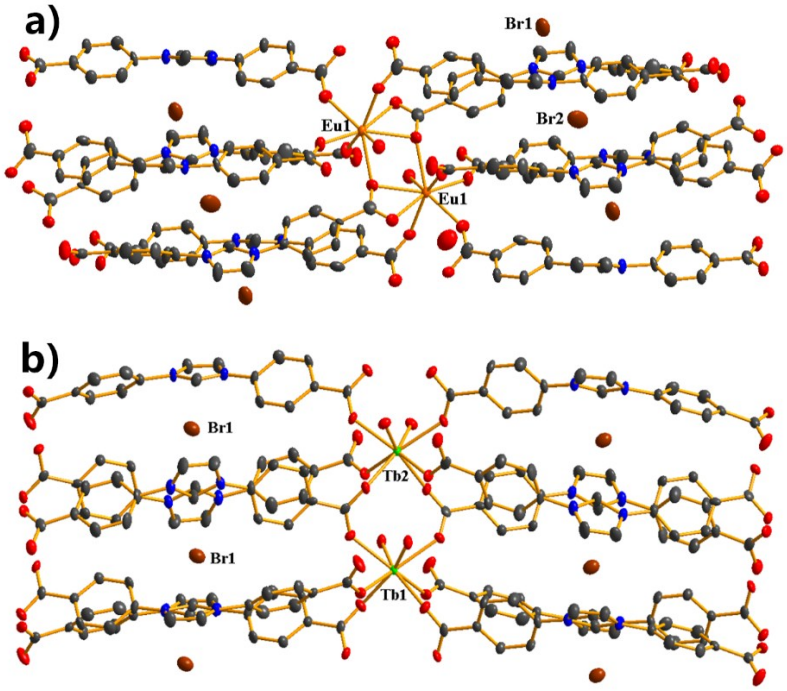

Figure S12. The ORTEP-style image of **a) EuBr** and **b) TbBr.**

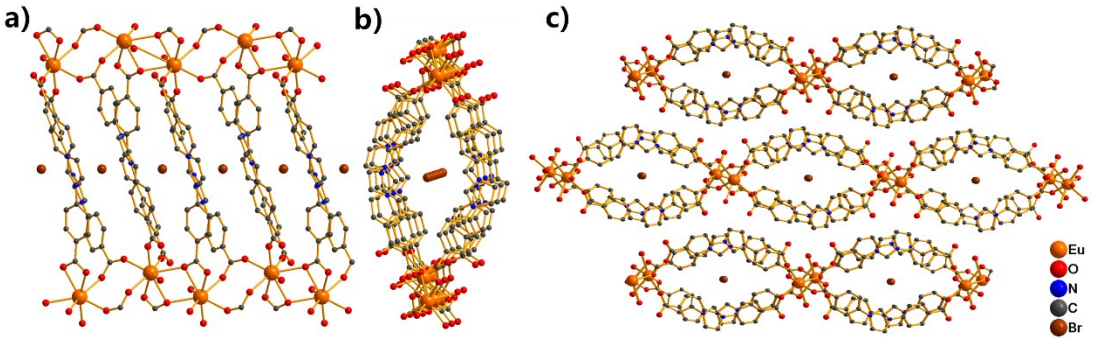

Figure S13. a) View of the 2D layer of **EuBr** along *b* axis direction. b) 1D channel of **EuBr** shown along *a* axis. c) Packing diagram along *a* axis showing three adjacent 2D layers.

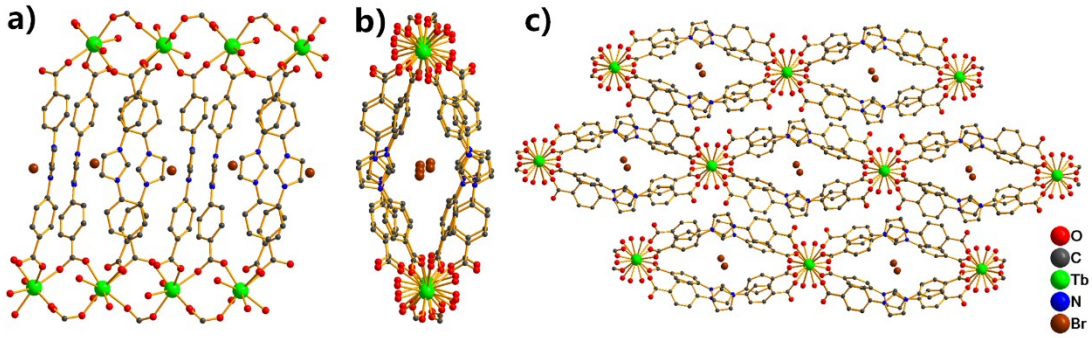

Figure S13. a) View of the 2D layer of **TbBr** along *a* axis direction. b) 1D channel of **EuBr** shown along *b* axis. c) Packing diagram along *b* axis showing three adjacent 2D layers.

Table S1. The Stern-Volmer equations and quenching effect constant (K_{sv}) of **EuBr** and **TbBr** for nitro-explosive analytes.

Analytes	Compound	Stern-Volmer equation	$K_{sv}(M^{-1})$
1,3-DNB	**EuBr**	$y = 3.3769x + 0.9483$, $R^2 = 0.9827$	3095
	TbBr	$y = 3.3266x + 0.9728$, $R^2 = 0.9903$	3356
2,4-DNT	**EuBr**	$y = 3.2715x + 0.9907$, $R^2 = 0.9976$	3171
	TbBr	$y = 2.5527x + 0.9823$, $R^2 = 0.9890$	2475
4-NT	**EuBr**	$y = 7.1303x + 0.9408$, $R^2 = 0.9922$	6755
	TbBr	$y = 9.3094x + 0.9471$, $R^2 = 0.9924$	8635
NB	**EuBr**	$y = 1.7992x + 1.0055$, $R^2 = 0.9919$	1830
	TbBr	$y = 2.4032x + 0.9975$, $R^2 = 0.9936$	2506
TNT	**EuBr**	$y = 2.5545x + 0.9899$, $R^2 = 0.9908$	2309
	TbBr	$y = 3.1032x + 0.9711$, $R^2 = 0.9909$	2976